IEEE Photonics Journal
An IEEE Photonics Society Publication

Open Access

Nonlinear Fiber Loop Mirror Optimization to Enhance the Performance of Multiwavelength Brillouin/Erbium-Doped Fiber Laser

Volume 6, Number 6, December 2014

A. W. Al-Alimi
M. H. Yaacob
A. F. Abas

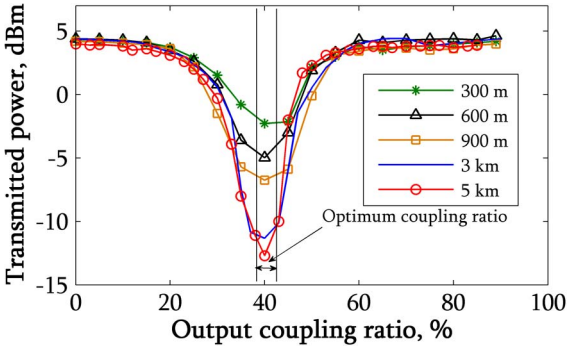

DOI: 10.1109/JPHOT.2014.2366171
1943-0655

IEEE photonics SOCIETY

IEEE

Nonlinear Fiber Loop Mirror Optimization to Enhance the Performance of Multiwavelength Brillouin/Erbium-Doped Fiber Laser

A. W. Al-Alimi,[1,2] M. H. Yaacob,[1,2] and A. F. Abas[1,2,3]

[1]Wireless and Photonic Networks Research Centre, Engineering and Technology Complex, Universiti Putra Malaysia, 43400 Serdang, Malaysia
[2]Photonics and Fiber Optic Systems Laboratory, Department of Computer and Communication Systems Engineering, Faculty of Engineering, Universiti Putra Malaysia, 43400 Serdang, Malaysia
[3]Department of Electrical Engineering, College of Engineering, King Saud University, Riyadh 11421, Saudi Arabia

DOI: 10.1109/JPHOT.2014.2366171

Manuscript received September 17, 2014; accepted October 13, 2014. Date of current version November 26, 2014. This work was supported in part by the Deanship of Scientific Research, Research Center, College of Engineering, King Saud University. Corresponding author: A. W. Al-Alimi (e-mail: mogni_66@yahoo.com).

Abstract: The performance of multiwavelength BEFL based on nonlinear fiber loop mirror (NOLM) optimization has been experimentally investigated. The NOLM is optimized to act as highly reflective mirror, which results in reducing the threshold power and enhancing the number of the generated Stokes lines at low EDF pump power as well. This design presents a low threshold power of 2 mW and generates up to 26 Stokes lines at EDF pump power of 25 mW.

Index Terms: Erbium-doped fiber, Brillouin fiber laser, stimulated Brillouin scattering, linear cavity, nonlinear fiber loop mirror.

1. Introduction

The performance of fiber laser source based on the nonlinearity effect such as stimulated Brillouin scattering (SBS), stimulated Raman scattering (SRS), and four wave mixing (FWM) that can generate a large number of Stokes lines has been discussed by many reports in the past [1]–[3]. The reported value of the wavelength spacing between the Stokes lines is around 10 GHz [4]. The SBS threshold power is also low. For instance, an efficient Brillouin fiber ring laser with low threshold power of 3.6 mW has been reported [5]. However, due to the low Brillouin gain in the single mode fiber (SMF), the number of Stokes lines is low. Therefore, to improve the Brillouin fiber laser operation efficiency, another gain medium is required. Two gain mediums were combined successfully in a ring cavity laser by Cowle and Stepanov in 1996 [4]. The combination of both gain medium in the same laser cavity realizes a Brillouin/Erbium fiber laser (BEFL). In this design, up to 6 Stokes lines was obtained at EDF pump power of 90 mW. In another ring cavity BEFL, up to 60 mW and 180 mW of EDF pump power were required for the first and for 24th Stokes line generation, respectively. Later, many different BEFL designs and different techniques have been proposed to improve threshold power and number of Stokes lines [6]–[12]. For example,

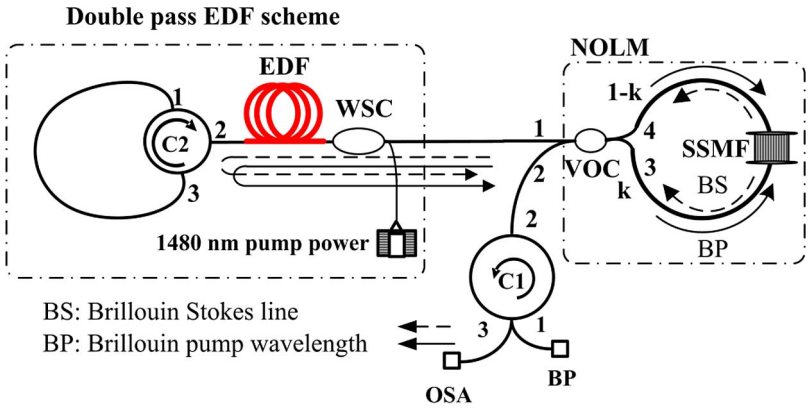

Fig. 1. Experimental setup of BEFL with NOLM.

the SBS threshold power can be improved by feeding back the generated Stokes lines into the laser cavity by utilizing reverse-S-shaped configuration [6]. More improvement was obtained by replacing the reverse-S-shaped fiber with broadband partially reflecting fiber Bragg grating [13]. Recently, 18 Stokes lines were obtained by employing a nonlinear optical loop mirror (NOLM) integrated with nonlinear polarization controller and quarter-wave-plate in ring cavity BEFL.

The linear cavity is another configuration, which was proposed to improve the performance of BEFL [14]. The linear cavity can be formed by utilizing two high reflective physical mirrors, which are fixed at both ends of the cavity. The physical mirror is an optical component and come in different form; circulator, high reflective mirror and 3-dB coupler [15]–[17]. Later, different techniques have been proposed to improve the linear cavity BEFL performance such as pre-amplified Brillouin pump (BP) power techniques [18]. In those designs, the BP power is amplified before being launched into the optical fiber, which resulted in the reduction of threshold power [7]–[12]. By utilizing this technique, up to 26 Stokes lines including BP wavelength were generated at EDF pump power of 90 mW and BP power of 3 dBm [19]. In the existing configurations of linear BEFL [6]–[12], besides the requirement of two physical mirrors, an additional coupler is needed for inserting the BP power into the laser cavity.

In general, the previous linear cavities BEFL require a high threshold power for the first and the subsequence Stokes lines. In other words, the generation of a large number of Stokes lines requires a high EDF pump power. This is due to the utilization of many optical components that drains most of the laser power. Therefore, the main challenge in designing an efficient BEFL configuration is to assure that the laser is able to generate a large number of Stokes lines with low EDF pump power. In this study, nonlinear fiber loop mirror (NOLM) was used as a high reflective physical mirror, as well as a coupler. As a result, the required optical components and EDF pump power are reduced.

In this paper, the experimental characterization results of linear cavity BEFL with NOLM are reported, which focuses on the threshold power, number of Stokes lines, and total output power of the generated Stokes lines. At the optimum condition, NOLM acts as a high reflective mirror. With EDF pump power of 25 mW, 26 Stokes lines were generated. More interestingly, this design has threshold power of as low as 2 mW.

2. Experimental Setup of BEFL With NOLM

The experimental setup of multiwavelength BEFL with NOLM is depicted in Fig. 1. The BEFL cavity structure is developed based on the double pass EDF structure that is connected to an NOLM. A circulator (C1) is used to provide the laser input and output ports. The double pass EDF structure consists of circulator (C2), wavelength selective coupler (WSC), 1480 nm pump power, and 10 m long EDF with absorption coefficient of 5.6 dB/m at 1531 nm.

The WSC is used to combine 1480 nm pump power and the oscillating signals. In this setup, C2 acts as a physical mirror. An external cavity tunable laser source (TLS) is used as the BP with maximum power of 4 mW and 200 kHz line width. The TLS can be tuned over a tuning range of 100 nm (1520 nm–1620 nm). An optical spectrum analyzer [20] with 0.01 nm resolution bandwidth is connected to port 3 of C1 to monitor the BEFL output spectrum.

3. Operation Principle of BEFL

The operation principle of the multiwavelength BEFL with NOLM can be described as follows: with the absence of the BP signal, the linear cavity works as a bidirectional EDFL. It experiences self lasing at the EDF peak gain wavelength. The linear cavity operates as BEFL when the BP signal was inserted into the laser cavity through port 1 of C1. Then, the BP signal was split into two parts by the NOLM. After that, each part of the BP signal enters the standard single mode fiber (SSMF). In this case, a narrow bandwidth gain is created inside the SSMF at a wavelength that is shifted from the incident BP wavelength. A large number of Stokes lines can be generated when the BP wavelength is tuned to be within or near the EDF peak gain region [21]. Both signals propagate inside the NOLM fiber loop and couple at the coupler. Small power of the inserted BP signal is transmitted into the double pass EDF scheme, where the BP signal is amplified twice, through port 1 of NOLM. Then, the amplified BP signal is reinjected into the NOLM. As EDF pump power increases, the circulated BP signal gains more power from EDF. The first Stokes line is appeared when the circulated BP signal has enough power to overcome the SBS threshold level. The first Brillouin Stokes line propagates in the opposite direction to the injected BP signal as illustrated in Fig. 1 (dash arrows in NOLM dash box) and down-shifted from BP wavelength by a value equal to $V_B = 2n\ v_a/\lambda_p$, where n is the refractive index of the SSMF, v_a is the acoustic velocity, and λ_p is the BP wavelength. When the first Stokes line power reaches SBS threshold level, it serves as BP signal to generate the second-order Stokes line. The generation of Stokes lines is continued until the power of the higher-order Stokes line becomes too weak to satisfy the SBS threshold condition. At the steady-state condition, a stable laser can be produced at port 3 of the C1, which is originated from the reflected BP and the generated Stokes signals. The requirement of BP power inside the NOLM to produce a new Stokes line can be represented by [22]

$$\frac{dP_{B_{P_n}}^{\substack{cw\\ccw}}(z)}{dz} = -\frac{g_B}{A_{eff}} P_{B_{P_n}}^{\substack{cw\\ccw}}(z) P_{S_n}^{\substack{cw\\ccw}}(z) \tag{1}$$

$$\frac{dP_{S_n}^{\substack{cw\\ccw}}(z)}{d_z} = -\frac{g_B}{A_{eff}} P_{B_{P_n}}^{\substack{cw\\ccw}}(z) P_{S_n}^{\substack{cw\\ccw}}(z) \tag{2}$$

where cw and ccw represent the clockwise and anti-clockwise Brillouin Stokes lines, respectively. The BP power that required to generate Stokes line inside the SSMF with power of $P_{S_n}^{cw/ccw}$ is represented by $P_{B_{P_n}}^{cw/ccw}$. Similarly, the $P_{S_n}^{cw/ccw}$ represents the power of the Stokes line to generate $(\mathrm{n}^{\mathrm{th}} + 1)$ Stokes line in clockwise or anti-clockwise direction. The g_B and the A_{eff} represent the Brillouin gain and effective length of SSMF, respectively.

In this experiment, the NOLM is used to determine the amount of the reflected power into the laser cavity and the amount of the transmitted power into the output port. At the optimum condition of the NOLM, in which most of the laser power is reflected, the BEFL performance in terms of SBS threshold power and the required EDF pump power to generate a large number of Stokes lines is improved. In comparison to the previously reported works [13], [23]–[25], the threshold power that is obtained from our experiment is lower.

4. Nonlinear Fiber Loop Mirror (NOLM) Characterization

The first NOLM configuration was proposed in 1988 by Doran and Wood [26]. Fig. 2 shows the basic NOLM configuration, which made up of a segment of an optical fiber and a coupler. The

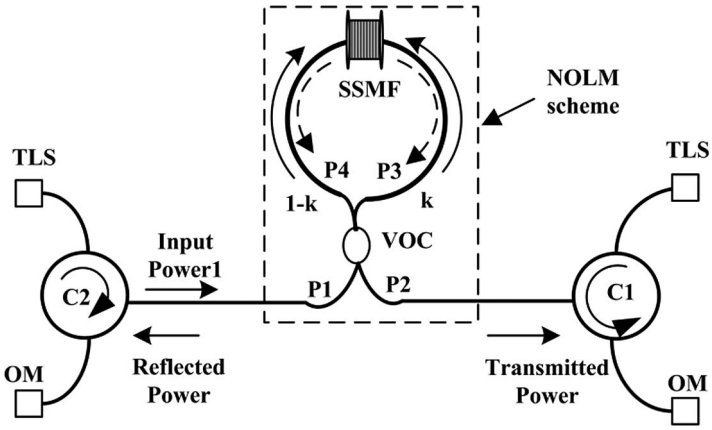

Fig. 2. Basic structure of NOLM.

coupler has two output ports with coupling ratio of (k) and (1-k). The NOLM is formed by connecting the output ports of the coupler with the fiber segment. This coupler splits the incident light into two counter propagating signals.

When the two signals propagate inside the fiber loop mirror, they accumulated phase shift. Then, they interfere again at the coupler, which is a variable optical coupler (VOC) in this experiment. Since the two signals propagate across the same optical fiber length with different powers, the phase shift, ϕ, of the two propagated signals can be expressed as [26]

$$\phi_1 = P_{in} L k \frac{2\pi n_2}{\lambda A_{eff}} \tag{3}$$

$$\phi_2 = P_{in} L (1-k) \frac{(2\pi n_2)}{\lambda A_{eff}} \tag{4}$$

where P_{in} is the input power, L is the loop length, n_2 is the refractive index coefficient, λ is the operating wavelength, and A_{eff} is the fiber effective area. The phase shift difference between the two counter-propagation signals during a round trip can be expressed as [26]

$$\Delta\phi = \phi_1 - \phi_2 = P_{in} L (1-2k) \frac{2\pi n_2}{\lambda A_{eff}}. \tag{5}$$

In general, the derived expression of the reflected and transmitted power of the NOLM can be expressed as [26]

$$P_{trans} = P_{in}(1 - 2k(1-k)(1 + \cos[(1-2k)\Delta\phi])) \tag{6}$$

$$P_{refl} = P_{in}(2k(1-k)(1 + \cos[(1-2k)\Delta\phi])). \tag{7}$$

Equations (6) and (7) present the impact of output coupling ratio of the NOLM, k, on the transmitted and reflected power. The NOLM output coupling ratio is represented by the parameter k [26]. This means that the two signals propagate inside the fiber with different intensity, which results in different phase shift. Thus, a nonlinear phase shift difference will be induced between the two signals.

The key elements in this characterization are the output coupling ratio of NOLM and SSMF length, which represents the fiber loop length and connects output ports of the NOLM (P3 and P4). In other words, the phase shift difference raising between the two signal can be minimized by adjusting SSMF, L, and output coupling ratio of the NOLM, k, as expressed in (5). Consequently, the reflected and transmitted powers of the NOLM can be controlled.

In the experiment, a wavelength of 1550 nm with power of 7 dBm generated from external tunable laser source was inserted into the port 1 of the NOLM through the input port 1 of the

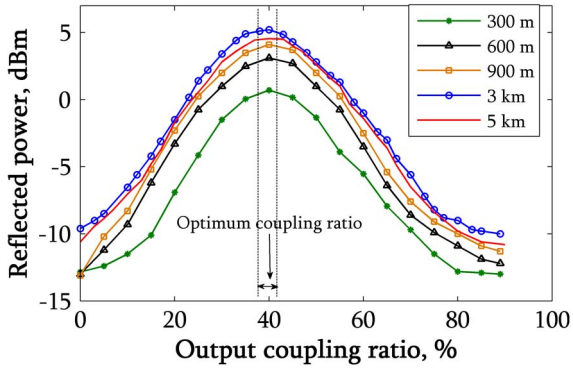

Fig. 3. Effect of output coupling ratio and loop length of NOLM on the reflected power of NOLM; the input power is 7 dBm.

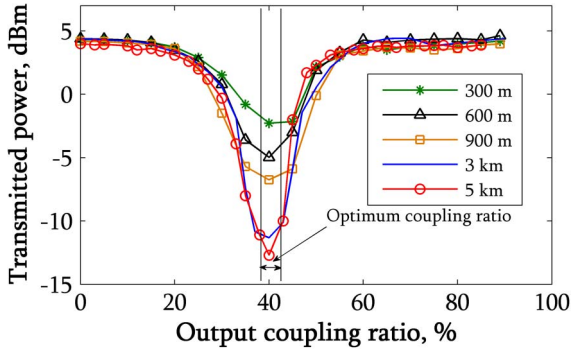

Fig. 4. Effect of output coupling ratio and fiber loop length of NOLM on the transmitted power of NOLM; the input power is 7 dBm.

circulator 2 (C2). The transmitted and reflected powers of the NOLM were measured by utilizing two optical power meters (OPMs) connected to port 3 of C1 and C2, respectively. In this characterization, different SSMF lengths were used; 300 m, 600 m, 900 m, 3 km, and 5 km. For each SSMF length, the transmitted and reflected powers of NOLM were recorded for output coupling ratio varying from 0% to 90%. Figs. 3 and 4 show the transmitted and reflected powers against output coupling ratio for different lengths of SSMF.

It can clearly be noticed that around output coupling ratio of 40%, the transmitted power decreases as the SSMF length is extended. In contrast, the reflected power is increased. This is due to the fact that the transmitted and reflected powers of the NOLM are originally based on phase difference between the counter propagating signals. This difference is due to the self-phase modulation (SPM) [26].

It is also can be clearly seen from Fig. 3 that the highest reflected power from NOLM can be obtained around output coupling ratio of 40% and SSMF length of 3 km. At 40% coupling ratio, the input signal is divided into two parts with approximately equal powers. Theoretically, in NOLM with 50% splitting ratio and neglecting the birefringence of the optical fiber in the loop, the two signals experience the same phase shift. Consequently, no signal transmitted to the output port of NOLM and all input signal reflected to the input. However, in practice case, due to the difficulties of having exactly 50% splitting ratio, a small power signal was transmitted into the output port of NOLM as shown in Fig. 4. In previous studies [15], [27]–[31], due to random birefringence of the optical fiber, which affects the phase shift of the propagated signal, a polarization controller [32], linear gain medium, quarter wave plate and attenuator were installed inside the NOLM to act as intensity equalizer, which results in minimize the phase shift difference

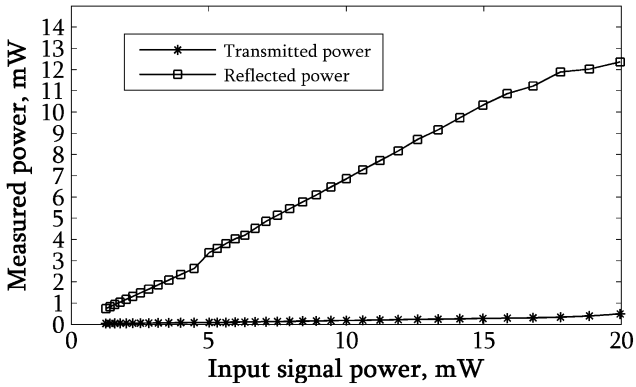

Fig. 5. The reflected and the transmitted powers of NOLM with output coupling ratio of 40% and 3 km SSMF against input signal power.

between the two propagated signals inside the NOLM. Consequently, NOLM with high reflectivity can be obtained. However, in this experiment, the output coupling ratio of the NOLM is adjusted to ensure that the input signal power is split equally into two parts. The fiber loop length of the NOLM is also adjusted to compensate the phase shift difference raising between the two signals. As a result, the need of installation of PC is removed. In general, the NOLM can be converted from high transmission to high reflection device by adjusting its design parameters such as output coupling ratio and fiber loop length.

Based on the previous NOLM characterization, the SSMF length of 3 km and coupling ratio of 40% make the NOLM to act as a high reflective mirror. Fig. 5 shows the transmitted and reflected powers of the NOLM with output coupling ratio 40% and SSMF length of 3 km as a function of input power. The input power of the signal is varied from 1.26 mW to 20 mW. The transmitted and reflected powers are measured at port 3 of C1 and C2, respectively. Fig. 5 shows that with output coupling ratio of 40%, as the input power increases, the transmitted and reflected powers of the NOLM increases. The reflected power increased from 0.74 mW to higher than 12.4 mW whereas the transmitted power increased from 0.04 mW to 0.5 mW as the input signal power increased from 1 mW to 20 mW. The loss of the power input is due to the passive losses of the NOLM, including loss of the VOC, loss of the circulator, and losses of fiber attenuation and fiber splices.

More recent studies have exploited the effect of NOLM as an effective component to improve the BEFL performance [15], [30]. In this study, the NOLM is used to reduce the SBS threshold power and the requirement of high EDF pump power.

5. Results and Discussion

In this work, the effect of fiber loop length of the NOLM on threshold power reduction is investigated as shown in Fig. 6. In this investigation, the BP power is varied from 0.69 mW to 4 mW and the output coupling ratio of the NOLM is fixed at 40%. It is clearly witnessed that as the optical fiber length is extended, the nonlinearity of the optical fiber is improved, which in turn reduce the SBS threshold to initialize the Brillouin scattering.

It is also noted that the threshold power that is required to generate the first Stokes line in the SSMF varied from 300 m to 900 m is higher for higher BP power. This is due to the fact that the inserted BP power into short SSMF determines the starting value of the Brillouin gain. Hence, it determines the threshold power of the first Stokes line [22]. In contrast, as SSMF is extended to beyond 900 m, the threshold power is inversely proportional to the BP power. This is due to fact that a small power from the BP power is transferred to the generated Stokes line. The transferred power is increased as the BP power increases, which results in reducing the SBS threshold. A low threshold power of 2 mW can be achieved by utilizing 3 km SSMF. However, due to

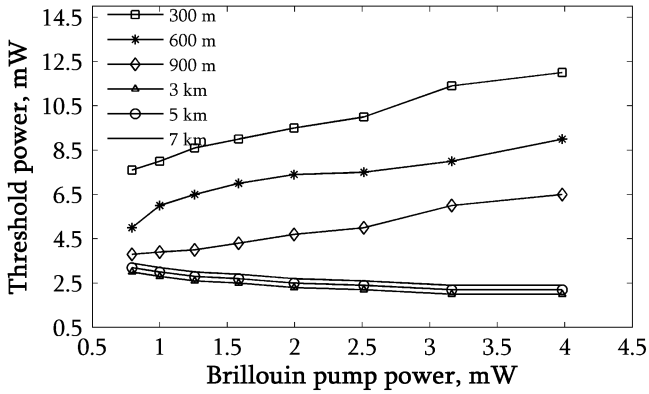

Fig. 6. BEFL threshold power against BP power for different SSMF lengths.

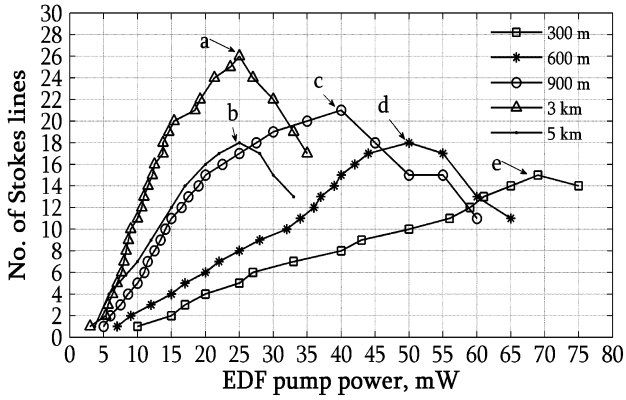

Fig. 7. The Stokes lines number against EDF pump power for different SSMF lengths.

the increase in the cavity loss, the BEFL threshold power is increased. This finding shows the effectiveness of the NOLM optimization in reducing SBS threshold.

Fig. 7 shows the effect of EDF pump power on the number of Stokes lines for different fiber loop lengths of the NOLM. For efficient BEFL performance, the BP power and wavelength must be optimized [4]. It is well known that the Brillouin gain of short SSMF is low; thus, strong BP power must be inserted into the BEFL cavity to improve the number of Stokes line and to eliminate the self lasing, particularly at high EDF pump power. From our observation, a high BP power of 4 mW is required for long SSMF varying from 300 m to 900 m. In contrast, a low EDF pump power of 0.87 mW is needed for SSMF longer than 900 m. The BP wavelength is also optimized for each fiber loop length to generate the maximum number of Stokes lines. In this investigation, the BP wavelength is fixed within EDF Peak gain of each SSMF length.

It is clearly shown that the requirement of high EDF pump power of 70 mW is reduced to 25 mW as the fiber loop length is extended from 300 m to 3 km. This is because the Brillouin gain as well as the reflected power increased as the SSMF length is extended to 3 km. Consequently, the amount of EDP pump and BP powers required to generate stable and large number of Stokes lines are increased. The markers (e, d, c, b, a) in Fig. 7 indicate to maximum number of Stokes that can be obtained by varying SSMF length from 300 m to 5 km. This result presents the effect of fiber loop length of the NOLM on the number of Stokes lines and the required EDF pump to generate stable Stokes lines. Up to 26 Stokes lines is obtained at EDF pump power of 25 mW, BP power of 0.89 mW and SSMF length of 3 km, which represents the highest number of Stokes line that can be achieved from this design. Fig. 8 presents the output spectrum of generated Stokes lines that can be obtained from this design with different SSMF lengths. The first

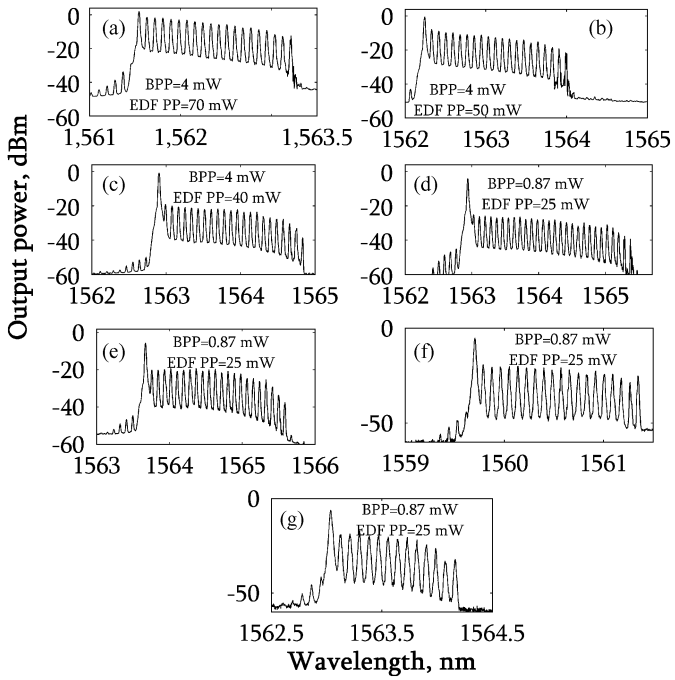

Fig. 8. Number of Stokes lines obtained from BEFL with different lengths of SSMF. (a) 300 m. (b) 600 m. (c) 900 m. (d) 3 km. (e) 5 km. (f) 7 km. (g) 10 km.

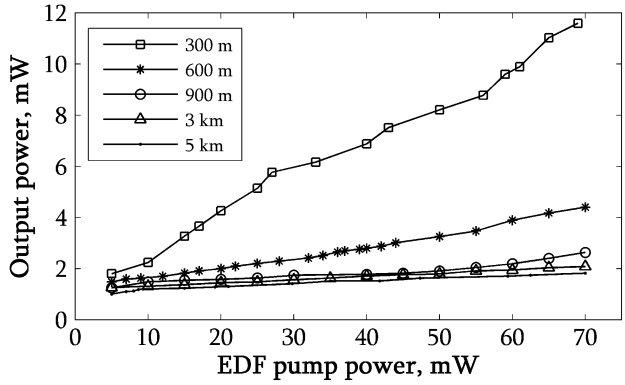

Fig. 9. The total output power of the generated Stokes lines against EDF pump power for different SSMF lengths.

line represents the BP signal, which has the higher peak power than the other Brillouin Stokes lines. This is attributed to the reflection and transmission features of the NOLM, as was clearly explained in the previous section.

Another important characteristic of multiwavelength BEFL is the total output power of BEFL. In this investigation, the OSA is used to monitor the BEFL output spectrum and measure the total output power of the generated Stokes lines. Fig. 9 depicts the total output power of the generated Stokes lines as a function of EDF pump power for different SSMF lengths; 300 m, 600 m, 900 m, 3 km, and 5 km. In this investigation, the BP power is fixed at 4 mW, while the EDF pump power is changed from 5 mW to 70 mW.

Although the BEFL with SSMF length of 300 m generates the least number of Stokes lines, as shown in Fig. 7, the highest BEFL output power is obtained at this short fiber length as compared with the other SSMF lengths. This is due to the fact that the SSMF length extension plays

a very important role on the phase shift difference reduction between the two signals, which results in decreasing the transmitted power of the NOLM [26].

It also is noted that the subsequence Stokes lines generation does not influence the reflectivity of the NOLM. This due to the fact that the Stokes line generation is basically generated from the incident BP signal and the wavelength spacings between the adjacent Stokes lines are nearly uniform and equal to $V_B = 2n\ v_a/\lambda_p$. Therefore, the phase shift difference between the nth-order clockwise (CW) and counter-clockwise (CCW) Stokes lines is equal to the phase shift difference between the original BP signals. Since the NOLM is characterized to avoid the imbalance power between the counter-propagating signals, the phase shift difference is very small. This also explains why the additional generations of Stokes lines with balance powers do not affect the interference condition.

In general, the total output power of the generated Stokes lines is decreased in tandem with fiber loop length of the NOLM and increased with the increasing of EDF pump power. At EDF pump power of 70 mW, the total output power is decreased from 11.6 mW to 1.8 mW as the length of SSMF is changed from 300 m to 5 km. Generally, in this BEFL configuration, up to 26 Stokes lines can be achieved with 3 km SSMF length at the expense of less output power of these generated Stokes signals. This is due to the dependence of the NOLM transmitted and reflected powers on the SSMF length, which plays an important role on the BEFL output power. Recently, a numerical study was deployed to study the effect of polarization controller, EDF pump power and quarter-wave-plate angle on the number of Stokes lines generation [33]. This module could be developed to expect the number of the generated Stokes lines in a linear cavity BEFL Structure.

5. Conclusion

A simple technique has been demonstrated to improve the BEFL performance in terms of threshold power and EDF pump power requirement for Stokes lines generation. The used technique is based on optimizing some design parameters of the NOLM: fiber loop length and output coupling ratio. It is found that recycling most of the BEFL power into the Brillouin gain results in SBS threshold reduction and enhance the number of Stokes lines at low EDF pump power. This finding will be very useful to the fiber laser designer in order to meet the industrial requirement for an economic and high performance multi wavelength laser source.

References

[1] R. Parvizi *et al.*, "Multi-wavelength Brillouin fiber laser using dual-cavity configuration," *Laser Phys. Lett.*, vol. 21, no. 1, pp. 205–209, Jan. 2011.
[2] Y. G. Han, J. H. Lee, S. B. Lee, L. Poti, and A. Bogoni, "Novel multiwavelength erbium-doped fiber and Raman fiber ring lasers with continuous wavelength spacing tunability at room temperature," *J. Lightw. Technol.*, vol. 25, no. 8, pp. 2219–225, Aug. 2007.
[3] A. Al-Alimi *et al.*, "150-channel four wave mixing based multiwavelength Brillouin-erbium doped fiber laser," *IEEE Photon. J.*, vol. 5, no. 4, Aug. 2013, Art. ID. 1501010.
[4] G. J. Cowle and D. Y. Stepanov, "Hybrid Brillouin/erbium fiber laser," *Opt. Lett.*, vol. 21, no. 16, pp. 1250–1252, Aug. 15, 1996.
[5] P. Zhang, S. Hu, S. Chen, Y. Yang, and C. Zhang, "A high-efficiency Brillouin fiber ring laser," *Chin. Opt. Lett.*, vol. 7, no. 6, pp. 495–497, Jun. 2009.
[6] N. M. Samsuri, A. K. Zamzuri, M. H. Al-Mansoori, A. Ahmad, and M. A. Mahdi, "Brillouin-erbium fiber laser with enhanced feedback coupling using common erbium gain section," *Opt. Exp.*, vol. 16, no. 21, pp. 16 475–16 480, Oct. 2008.
[7] M. H. Al-Mansoori, M. A. Mahdi, and A. K. Zamzuri, "Tunable multiwavelength Brillouin-erbium fiber laser with intra-cavity pre-amplified Brillouin pump," *Laser Phys. Lett.*, vol. 5, no. 2, pp. 139–143, Feb. 2008.
[8] M. N. M. Nasir, Z. Yusoff, M. H. Al-Mansoori, H. A. A. Rashid, and P. K. Choudhury, "Widely tunable multi-wavelength Brillouin-erbium fiber laser utilizing low SBS threshold photonic crystal fiber," *Opt. Exp.*, vol. 17, no. 15, pp. 12 829–12 834, Jul. 2009
[9] S. Shahi, S. W. Harun, N. S. Shahabuddin, M. R. Shirazi, and H. Ahmad, "Multi-wavelength generation using a bismuth-based EDF and Brillouin effect in a linear cavity configuration," *Opt. Laser Technol.*, vol. 41, no. 2 pp. 198–201, Mar. 2009.
[10] M. H. Al-Mansoori and M. A. Mahdi, "Reduction of gain depletion and saturation on a Brillouin-erbium fiber laser utilizing a Brillouin pump preamplification technique," *Appl. Opt.*, vol. 48, no. 18, pp. 3424–3428, Jun. 2009.
[11] M. H. Al-Mansoori, M. K. Abd-Rahman, F. R. M. Adikan, and M. A. Mahdi, "Widely tunable linear cavity multiwavelength Brillouin-erbium fiber lasers," *Opt. Exp.*, vol. 13, no. 9, pp. 3471–3476, May 2005.

[12] Z. Abd Rahman *et al.*, "Optimization of Brillouin pump wavelength location on tunable multiwavelength BEFL," *Laser Phys. Lett.*, vol. 19, no. 11, pp. 2110–2114, Nov. 2009.
[13] M. I. Johari *et al.*, "Ring cavity multiwavelength Brillouin-erbium fiber laser with a partially reflective fiber Bragg grating," *J. Opt. Soc. Amer. B, Opt. Phys.*, vol. 26, no. 9, pp. 1675–1678, Sep. 2009
[14] M. H. Al-Mansoori, B. Bouzid, B. M. Ali, M. K. Abdullah, and M. A. Mahdi, "Multi-wavelength Brillouin-erbium fibre laser in a linear cavity," *Opt. Commun.*, vol. 242, no. 1–3, pp. 209–214, Nov. 2004.
[15] M. H. Al-Mansoori and M. A. Mahdi, "Broadly tunable L-band multiwavelength BEFL utilizing nonlinear amplified loop mirror filter," *Opt. Exp.*, vol. 19, no. 24, pp. 23 981–23 988, Nov. 2011.
[16] M. M. Nasir, Z. Yusoff, M. Al-Mansoori, H. A. Rashid, and P. Choudhury, "Low threshold and efficient multi-wavelength Brillouin-erbium fiber laser incorporating a fiber Bragg grating filter with intra-cavity pre-amplified Brillouin pump," *Laser Phys. Lett.*, vol. 6, no. 1, pp. 54–58, Jan. 2009.
[17] M. H. Al-Mansoori, M. Ajiya, and M. A. Mahdi, "L-band multiwavelength BEFL with amplified fiber loop mirror," *IEEE Photon. J.*, vol. 4, no. 2, pp. 483–490, Apr. 2012.
[18] M. H. Al-Mansoori and M. A. Mahdi, "33-channels multiwavelength generation of L-band Brillouin-erbium fiber laser," presented at the Eur. Conf. Lasers Electro-Optics/Eur. Quantum Electron. Conf., Munich, Germany, 2009, Paper CJ_P14.
[19] M. Nasir, Z. Yusoff, M. H. Al-Mansoori, H. A. A. Rashid, and P. K. Choudhury, "Multi-wavelength Brillouin-erbium fiber laser utilizing a fiber Bragg grating filter with intra-cavity pre-amplified Brillouin pump," in *Proc. 6th NCTT/2nd MCP*, 2008, pp. 174–177.
[20] S. Rota-Rodrigo *et al.*, "Multiwavelength fiber ring laser based on optical add-drop multiplexers and a photonic crystal fiber Sagnac interferometer," *Opt. Laser Technol.*, vol. 48, pp. 72–74, Jun. 2013.
[21] D. Y. Stepanov and G. J. Cowle, "Properties of Brillouin/erbium fiber lasers," *IEEE J. Sel. Topics Quantum Electron.*, vol. 3, no. 4, pp. 1049–1057, Aug. 1997.
[22] D. Stepanov and G. Cowle, "Modelling of multi-line Brillouin/erbium fibre lasers," *Opt. Quantum Electron.*, vol. 31, no. 5–7, pp. 481–494, Jul. 1999.
[23] M. N. Mohd Nasir, Z. Yusoff, M. H. Al-Mansoori, H. A. Abdul Rashid, and P. K. Choudhury, "Low threshold and efficient multi-wavelength Brillouin-erbium fiber laser incorporating a fiber Bragg grating filter with intra-cavity pre-amplified Brillouin pump," *Laser Phys. Lett.*, vol. 6, no. 1, pp. 54–58, Jan. 2009.
[24] J. Zhao, T. Liao, X. Yang, Z. Tong, and Y. Liu, "A simple tunable multiwavelength Brillouin-erbium fiber ring laser with low threshold power," *J. Opt.*, vol. 12, no. 11, Nov. 2010, Art. ID. 115202.
[25] N. A Malini *et al.*, "Investigation on the effect of EDFA location in ring cavity Brillouin-erbium fiber laser," *Opt. Exp.*, vol. 17, no. 14, pp. 11 768–11 775, Jul. 2009.
[26] N. J. Doran and D. Wood, "Nonlinear-optical loop mirror," *Opt. Lett.*, vol. 13, no. 1, pp. 56–58, Jan. 1, 1988.
[27] X. P. Dong, L. Shenping, K. S. Chiang, M. N. Ng, and B. C. B. Chu, "Multiwavelength erbium-doped fibre laser based on a high-birefringence fibre loop mirror," *Electron. Lett.*, vol. 36, no. 19, pp. 1609–1610, Sep. 2000.
[28] L. Y. Wook, J. Jung, and L. Byoungho, "Multiwavelength-switchable SOA-fiber ring laser based on polarization-maintaining fiber loop mirror and polarization beam splitter," *IEEE Photon. Technol. Lett.*, vol. 16, no. 1, pp. 54–56, Jan. 2004.
[29] V. Marembert, "Investigations on ultrafast fiber-based optical gates," Ph.D. dissertation, Universitätsbibliothek, Heidelberg, Germany, 2006.
[30] M. H. Al-Mansoori and M. A. Mahdi, "Multiwavelength L-band Brillouin erbium comb fiber laser utilizing nonlinear amplifying loop mirror," *J. Lightw. Technol.*, vol. 27, no. 22, pp. 5038–5044, Nov. 2009.
[31] A. W. O'Neill and R. P. Webb, "All-optical loop mirror switch employing an asymmetric amplifier/attenuator combination," *Electron. Lett.*, 26, no. 24, 2008–2009, Nov. 1990. [Online]. Available: http://digital-library.theiet.org/content/journals/10.1049/el_19901298
[32] P. Reeves-Hall and J. Taylor, "Wavelength tunable CW Raman fibre ring laser operating at 1486-1551 nm," *Electron. Lett.*, vol. 37, no. 8, pp. 491–492, Apr. 2001.
[34] Y. Yuan, Y. Yao, M. Yi, B. Guo, and J. Tian, "Multiwavelength fiber laser employing a nonlinear Brillouin optical loop mirror: Experimental and numerical studies," *Opt. Exp.*, vol. 22, no. 13, pp. 15 352–15 363, Jun. 30, 2014.